One-Pot Assembly of a Hetero-dimeric DNA Origami from Chip-Derived Staples and Double-Stranded Scaffold

Alexandria N. Marchi,[†,#] Ishtiaq Saaem,[†,‡,#] Jingdong Tian,[†,‡] and Thomas H. LaBean[†,§,⊥,¶,*]

[†]Department of Biomedical Engineering [‡]Institute for Genome Sciences and Policy [§]Department of Computer Science [⊥]Department of Chemistry, Duke University, Durham, North Carolina 27708, United States, and [¶]Materials Science & Engineering Department, North Carolina State University, Raleigh, North Carolina 27606, United States. [#]These authors contributed equally and are to be considered cofirst authors.

ABSTRACT Although structural DNA nanotechnology, and especially scaffolded DNA origami, hold great promise for bottom-up fabrication of novel nanoscale materials and devices, concerns about scalability have tempered widespread enthusiasm. Here we report a single-pot reaction where both strands of double-stranded M13-bacteriophage DNA are simultaneously folded into two distinct shapes that then heterodimerize with high yield. The fully addressable, two-dimensional heterodimer DNA origami, with twice the surface area of standard M13 origami, formed in high yield (81% of the well-formed monomers undergo dimerization). We also report the concurrent production of entire sets of staple strands by a unique, nicking strand-displacement amplification (nSDA) involving reusable surface-bound template strands that were synthesized *in situ* using a custom piezoelectric inkjet system. The combination of chip-based staple strand production, double-sized origami, and high-yield one-pot assembly markedly increases the useful scale of DNA origami.

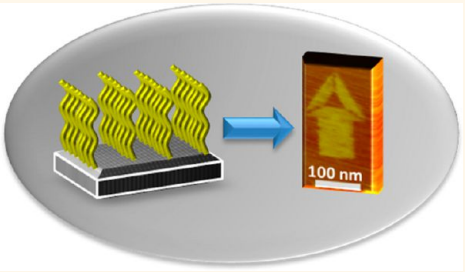

KEYWORDS: structural DNA nanotechnology · molecular self-assembly · DNA origami · chip-synthesized oligonucleotides · synthetic biology · gene-synthesis · inkjet

DNA nanotechnology is an emerging field focused on engineering self-assembled, nanostructured materials from nucleic acid building blocks and using these novel materials for a variety of applications.[1−5] Specifically, the advent of scaffolded DNA origami has allowed for the formation of complex nanostructures with uniquely addressable features and sub-10 nm resolution.[6−10] The one-pot origami method uses numerous short oligonucleotides (staple strands) to direct folding of a larger template (scaffold) DNA strand. The length of the scaffold strand limits the scale and ultimately the addressable surface area of these structures. A number of approaches have been examined for expanding the available surface area of the DNA construct, including multiple use of identical scaffolds,[11] substitution of DNA tiles in place of simple, linear staples,[12] and utilization of a double-stranded (dsDNA) scaffold.[13] These previous strategies suffered several limitations including low assembly yields or loss of unique addressability. During the preparation of this manuscript, a 26 kilobase origami was reportedly assembled using scaffold strand PCR amplified from a segment of the lambda phage genome; however both the scaffold purity and the assembly yield were quite low, leading to low quality origami.[14] The methods described herein successfully overcome all of these previous limitations, while increasing the uniquely addressable space with 81% dimerization yield in a one-pot assembly.

To maintain unique addressability, an increasing number of distinct staple strands must be utilized as the size of the origami increases. Although the cost of solid-phase chemical synthesis of DNA has drastically decreased in the past decade, excessive cost can still inhibit the design and construction of larger scaffolded DNA origami structures due to the considerable number of staple strands needed.[15] Exhaustive studies of structure formation and scaling to greater complexity could be facilitated using low-cost DNA chip[16] and gene-synthesis technology[17,18] to generate both staple

* Address correspondence to thlabean@ncsu.edu.

Received for review May 25, 2012 and accepted January 2, 2013.

Published online January 02, 2013
10.1021/nn302322j

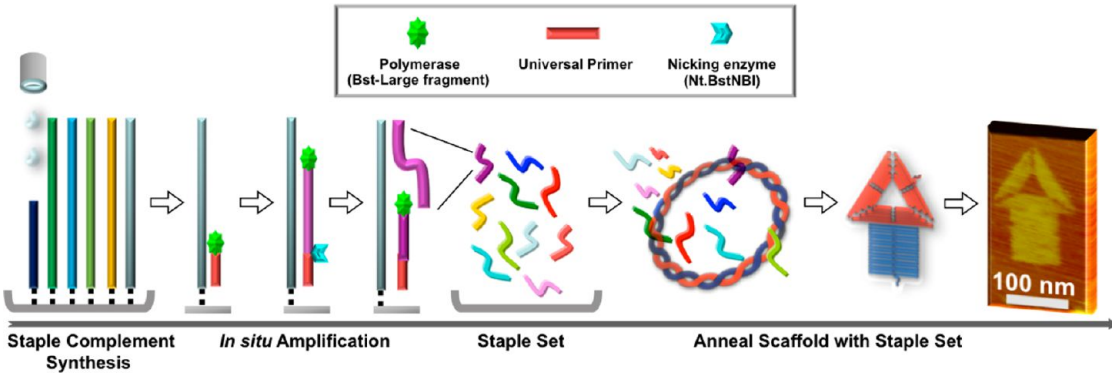

Figure 1. Outline for forming 14 Kbp DNA origami from chip-derived oligonucleotides. Staple complement versions of the desired staples, appended with a universal 25-mer linker/primer-binding-site, were synthesized on-chip. During the *in situ* amplification, a DNA polymerase (Bst-Large fragment, shown in green) extends and displaces the preceding strand while a nicking endonuclease (Nt.BstNBI, shown in blue) separates the staple from the universal primer (in red) and generates new 3′-ends for the next round of extension. After amplification, the staple set was collected and annealed with the scaffold to form DNA origami. The two strands of the double-stranded M13 scaffold were folded to create two distinct structures that were then brought together during an extended incubation to form the double-sized, heterodimer origami structure.

and scaffold strands. As a first step toward such a goal, we demonstrate in this report that both strands of a biologically derived, double-stranded M13 scaffold can be simultaneously folded by chip-derived staple strands to form DNA origami nanostructures. Double-stranded DNA scaffold strands were dissociated by a combination of thermal and chemical-denaturation[13] and preferentially reassociated with staples encoding two unique structures (rectangles and triangles) that are then unified (into "nano-houses") in a one-pot reaction. With additional incubation for 12 h at 35 °C after the initial anneal, over 80% of the well-formed origami monomers coalesce into the intended heterodimer final structure as analyzed by AFM. We anticipate that the presented strategy will enable mass production of even larger DNA origami designs at high yields.

RESULTS/DISCUSSION

Staple strands were generated from surface-bound oligonucleotides on DNA chips and used to anneal double-stranded scaffold as shown in Figure 1. Initially, the staple complements appended with a universal 25-mer linker were synthesized by phosphoramidite chemistry using an inkjet DNA synthesizer[16,19−21] on thermoplastic microarray slides functionalized with deposited silica thin films.[18,22] Subsequently, nicking-strand displacement amplification (nSDA) was performed on-chip using a nicking endonuclease (nickase) and a strand-displacing thermophilic DNA polymerase (see Methods section) to linearly amplify and generate the requisite staple set. The staple sets synthesized for this report spanned from 13-mers to 48-mers and were synthesized on a chip containing 3 456 discrete features, allowing for 384 unique sequences with a 9-feature redundancy. Previously, a similar chip has been shown to allow synthesis of 85-mer oligonucleotides at a cost of <$30/chip.[20] Considering a staple oligo to be an average length of 40 bases, approximately 15 360 polymerized bases are yielded from a chip. The total cost of oligo synthesis per chip, including phosphoramidites, other synthesis chemicals, organic solvents, gases, and the cyclic olefin copolymer (COC) chip, is still under $30. Therefore, the estimated cost of chip-oligonucleotide synthesis would be less than $30/15 360 bases = $0.00195/base of final synthesized sequences. Additional cost after oligo microarray synthesis comes from enzymatic reactions for oligo amplification (nSDA). The total reaction volume on a chip containing 8 subarrays is 50 μL × 8 = 400 μL. The estimated cost of all reagents needed for nSDA, including enzymes, dNTPs, and buffers, is approximately $20 per chip. Therefore, the estimated total cost of staple synthesis would be less than $(30 + 20)/15 360 bases = $0.00326/base of final synthesized strands. Sourcing oligonucleotides from chips represents the cheapest alternative to bulk-synthesis provided by commercial entities such as IDT. As highlighted by Borovkov *et al.*,[39] commercial sources for chip-derived oligonucleotides are available, and their material is cheaper by greater than 2 orders of magnitude. In our work, we utilized a 9-feature redundancy instead of maximizing unique species in order to ensure representative yield of all 384 sequences. However, without deep next-generation sequencing, single species yield statistics are difficult to glean based solely on origami formation. In this report, amplified product was pooled, purified using either phenol chloroform extraction or an enzyme removal resin[23] to remove proteins and excess nucleotides, and used for annealing with a biologically derived, dsDNA M13 scaffold that had been linearized *via* restriction enzyme digestion. The scaffold was folded to form only rectangles, only triangles, rectangles and triangles simultaneously, or a `nanohouse' structure by interconnecting a rectangle and a triangle *via* protruding staple strands on one origami edge (helical side, as opposed to helix ends)

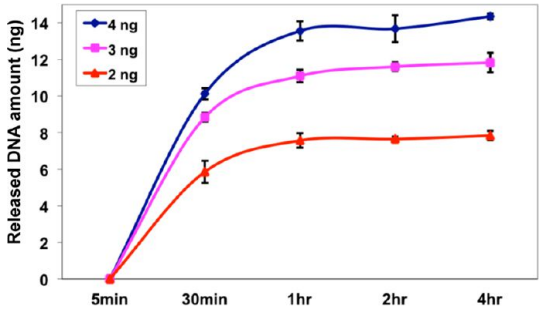

Figure 2. Assessment of *in situ* amplification in releasing amplified product. The reaction, a nicking strand displacement amplification (nSDA) process driven by a nickase and polymerase, was assessed using varying amounts of starting DNA that serve as the amplification template (where the template is the reverse complement of the desired sequence). Data were gathered by running incubation product on polyacrylamide gels followed by image analysis to determine target band fluorescence in comparison to a known low mass DNA ladder. Each data point represents the mean of three trials where the error-bars represent standard deviation.

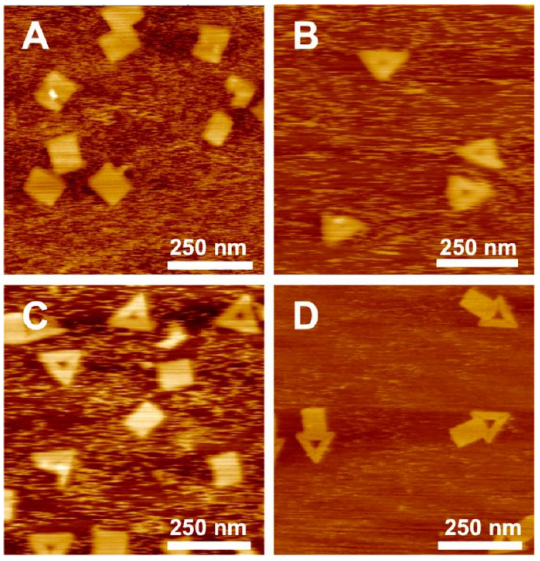

Figure 3. Formation of DNA origami structures using a double-stranded scaffold employing a formamide annealing process. Individual, single monomers (A and B) or two simultaneous, discrete monomers (C) can be formed using either a solitary staple set or two combined sets, respectively, in the 90-min anneal process. Using a combined staple set that contained modified connector staples, triangular and rectangular structures were simultaneously formed and joined to form a heterodimer structure (D).

that bind the scaffold strand of the opposite structure, forming heterodimers. For the formation of the nanohouse, an extended incubation period (in the same microfuge tube, without adding any new reagents) boosted yield appreciably.

To ascertain amplification rates on-chip *via* nSDA, a control 73-mer sequence (see Methods section) was synthesized on 100, 75, or 50 array features on a chip subarray. During the amplification reaction, DNA polymerase (Bst large fragment) generated the intended staple strand from its synthesized, complementary template by extending a primer and simultaneously displacing the previously synthesized strand. Concurrently, a nicking endonuclease (Nt.BstNBI) cleaved the newly synthesized oligo and separated the intended staple strand from the universal primer, thus generating new 3′-ends for extension. After amplification, a 48-mer sequence was released and subsequently quantified by gel analysis as presented in Figure 2. On the basis of our previous analysis of material release from each array feature,[16] it was calculated that approximately 4, 3, and 2 ng of template (from 100, 75, or 50 array features, respectively) was present on-chip, yielding a 4-fold amplification *via* nSDA. To gauge the life span of a chip, we carried out 10 sequential amplification reactions on a chip bearing templates for the triangle origami staple strand set. Product strands from each amplification reaction were successful in folding single-stranded scaffold into the expected object, thus demonstrating that the synthesized, on-chip DNA libraries can be stored in a freezer and then repeatedly recalled for use as template for staple strand production. Recently, Joneja *et al*., Tan *et al*., and Kucera *et al*. reported a strand displacement amplification (SDA) initiated by a nickase similar to the reaction described here.[24−26] Their experiments, carried out in solution, produced a 10-fold higher amplification yield, indicating that our on-chip amplification step may be limited by surface interactions, mass transport issues near the surface, and possibly by inhibition due to nonspecific adsorption. Additionally, the nSDA system could utilize different initiating primers instead of a universal priming sequence. Such a modification would allow for release off of a designated chip region and the corresponding subset staple pool. When designing different initiation primers, appropriate nickase binding regions must be included and the sequence should be of the highest orthogonality possible, given the staple pool design. Both the above represent areas for further optimization and future work that could increase the yield of chip-based oligonucleotide from single subarrays enabling sufficient yields after a single round of amplification rather than requiring multiple rounds of amplification and pooling from multiple subarrays, as was done in this study. It would also allow for selective amplification of only the necessary strands for a particular assembly. Staple pool concentrations in this study were additionally quantified *via* UV absorption spectroscopy as detailed in Supporting Information, section S1.

Pools of oligos harvested from the chip were designed to fold either the M13 single-stranded phage or both strands of the double-stranded M13 phagemid into nanostructures resembling the tall rectangle or sharp triangle from Rothemund's original DNA origami paper.[6] The M13 double-stranded scaffold was cut at a single restriction site by the restriction endonuclease

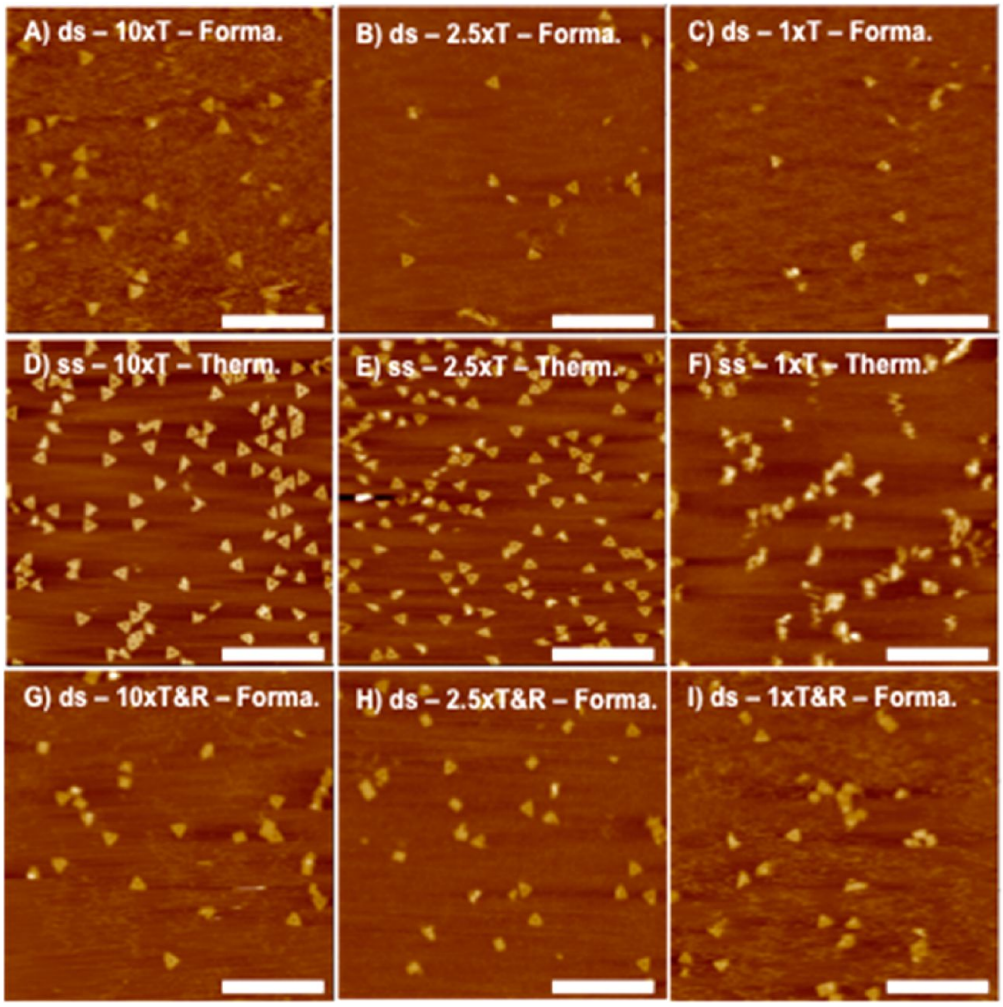

Figure 4. Comparison, by AFM imaging, of origami formation employing a formamide anneal with double-stranded scaffold or a thermal anneal with single-stranded scaffold while decreasing the concentration of staple strands relative to scaffold strands. Using decreasing amounts of the origami staple sets (10×, 2.5×, 1× relative to the double-stranded scaffold) and employing a formamide-assisted anneal, some discernible structures were seen even at 1× staple concentration (top and bottom rows). However, upon thermal annealing with the single-stranded scaffold (middle row), indeterminate structures were seen at 1× staple concentration (F). Scale bars are 1 μm.

*Eco*RI. Each strand from the scaffold was folded into either a rectangle or triangle using a staple strand pool composed of hundreds of unique sequences (Supporting Information, section S3). As strictly thermal anneals were not sufficient for DNA origami formation on the double-stranded scaffold, we employed a chemical denaturant based annealing strategy originally reported for isothermal origami formation with single-stranded DNA scaffold by Jungmann *et al.*[27] and further used for double-stranded scaffold assembly by Högberg *et al.*[13] Formamide, a small molecule that interferes with hydrogen bonding between base pairs, was used as a chemical denaturant to assist in separation of the two long, complementary scaffold strands and to control base pair formation between scaffold and staple strands. The optimal annealing protocol included heating the components to 80 °C in 40% formamide for 10 min followed by a quick cooling step to room temperature, which was necessary to avoid scaffold−scaffold interactions and tangling. Then, the samples were dialyzed to 0% formamide in six, 10-min steps. The thermal and chemical contributions to denaturation are combined to estimate an "effective temperature" of the reaction since formamide lowers the actual melting temperature of double-stranded DNA by ~0.64 °C for each 1% formamide present (Supporting Information, section S1).[36−38] Gel electrophoresis studies demonstrated that our chosen thermochemical annealing conditions (80 °C with 40% formamide) provided optimal origami formation (Supporting Information, section S1). AFM imaging further demonstrated the assembly of both sharp triangles and tall rectangles using the double-stranded M13 scaffold as shown in Figure 3. When the staple pool encoded a single structure, the expected origami shapes were observed (Figure 3A,B). In Figure 3C, where the staple pool contained both sets of staple strands, triangle and rectangle origami can be observed as

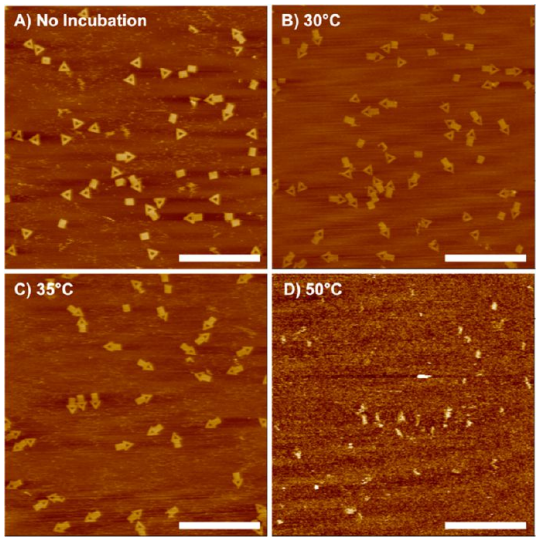

Figure 5. Formation of nanohouse DNA origami structures with improved yields using an extended postassembly anneal. The population of well-formed structures increased when, following initial assembly (A), the sample was further incubated for 12 h at 30 °C (B). The highest yield of the desired structure was achieved at 35 °C (C). A low yield was observed where the component structures disintegrated after incubation at 50 °C (D). Scale bars are 1 μm.

separate monomers. Since we desired larger origami structures with the same specific addressability and pixel resolution, we modified the staple sequences of the triangle and rectangle staple strands to include strands that bridge between the scaffold strands and attach the two structures to one another. This resulted in the formation of a heterodimeric nanohouse structure from a one-pot reaction (Figure 3D).

Reannealing of the long complementary M13 scaffold strands is favored thermodynamically over formation of the origami structures *via* staple-scaffold binding, and it had been thought that both a denaturant annealing strategy and a 10-fold molar excess of staple strands (*i.e.*, where the staple to scaffold ratio is 10:1) are key for origami formation from a double-stranded scaffold.[13] To further investigate this process, we varied the amount of staple strands by using either 10-fold or 2.5-fold molar excess or an equimolar mixture of staple strands *versus* scaffold strand during thermal/formamide anneals. We recognize that measurements of scaffold and staple strand concentrations are subject to differing sources of experimental error, and therefore the molar ratios stated here should be viewed as best estimates. Upon AFM imaging, we were able to observe a large population of representative structures for the 10-fold and 2.5-fold conditions with both single-stranded and double-stranded scaffold thermal and formamide anneals (see columns one and two of Figure 4).

Similar to Rothemund's original observations,[6] thermal anneals of a single-stranded scaffold with approximately equimolar mixtures of staple strands did not produce high-quality structures. However, formamide anneals folding one or both of the scaffold strands

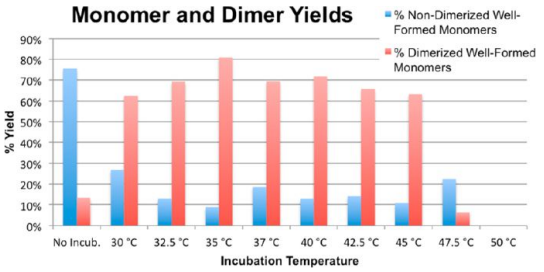

Figure 6. Formation yields quantified by counting structures in AFM images. The blue bars represent the yield of nondimerized, well-formed monomers (count of well-formed monomers not in dimers, divided by the total count of all monomers observed, whether dimerized or not). The dimerization yield (red bars) is the proportion of well-formed monomers observed to participate in dimers.

from double-stranded M13 with approximately equimolar staple sets did produce a small population of well-formed structures. These results show that consideration of an appropriate annealing strategy (chemical and thermal) is necessary for efficient assembly of intact nanostructures when staple sets and scaffold strands increase in complexity. In forming the nanohouse structure, we used an approximately equimolar amount of linker strands connecting the rectangle and triangle to the scaffold strands forming the structures. If the normal formamide anneal procedure was followed, the yield of interconnected two-part nanostructure was fairly low. As shown in Figure 5A, although representative nanohouses are observed, the majority of the structures are disconnected rectangular and triangular monomers. We reasoned that the linking staples would have an increased probability of binding to both scaffolds of the triangle and rectangle structures given a longer incubation time. Therefore, we incubated the product of the initial formamide assembly for 12 h at varying temperatures and examined structure formation (Supporting Information, sections S1 and S2). We found that the highest population of well-formed nanohouse structures were observed *via* AFM imaging (Figure 5C) by an extended incubation at 35 °C. Yields of structure formation were determined by counting structures as observed on AFM images (see Supporting Information, section S2 for details). The highest yield of well-formed monomers observed to undergo dimerization was 81% at 35 °C, and, for anneals with observable structure formation, the lowest dimerization yield was achieved for the anneal with the extended incubation at 47.5 °C (Figure 6 and Supporting Information, Table S1). Our dimerization yield is slightly lower than the 91% rate of monomer conversion into dimers from previous studies by Woo *et al*. where monomeric structures, formed in separate tubes by folding single-stranded M13, were then mixed and dimerized based on helical stacking and shape matching, rather than by sticky end or staple bridging between shapes.[28] In contrast, here we folded two distinct sequences and formed two distinct shapes

in a one-pot assembly method. In further comparison to previous studies that show dimerization of structures formed from the single-stranded M13,[29,30] the staple sets of our individual monomers differ completely because of the different scaffold sequence being folded. This eliminates the necessity for separate monomer formation, staple filtration, and sample mixing during the assembly process.

Interestingly, all structures disintegrated when the extended incubation temperature was increased by 15 °C. Although the lowest melting temperature of the designed staple strands was greater than 50 °C as predicted by Mfold,[31] extended incubation at 50 °C destabilized the thermodynamic balance of origami formation. This seemingly contradicts a previous report by Liu *et al.*[32] where two individually formed origami structures were brought together to form 2-dimensional arrays with an optimal temperature of 53 °C. Liu *et al.* also showed intact origami structures that underwent incubations at 65 °C. However, the lower assembly temperature observed for our system is likely due to differences between the constructs (Liu *et al.* used larger lattices and monomer interfaces involving helix stacking), as well as competition in our system between origami formation *via* staple-scaffold binding *versus* rehybridization of the double-stranded scaffold.

CONCLUSION

We have demonstrated a number of interesting advancements for DNA origami. First, templates for amplification that are complementary to desired staple strands can be synthesized *in situ* on a DNA chip and subsequently used repeatedly in nSDA reactions to produce staple sets directly on the chip surface. Second, such staple pools can be used to fold both strands of a double-stranded DNA phagemid into two distinct nanometer-scale objects or into an interconnected two-part structure that is still uniquely addressable. Finally, the combination of chip-derived staple strands and double-stranded scaffold presented here is an important step toward the production of larger origami projects (*e.g.*, requiring thousands of staple strands) and exhaustive studies of structure formation that have thus far been difficult because of the prohibitive cost of oligo synthesis. The use of DNA nanostructures for the organization of inorganic nanomaterials holds great promise for the bottom-up fabrication of functional electronic and photonic devices.[33] Additionally, the advent of gene synthesis from chips could enable the synthesis of a completely artificial scaffold for use in DNA nanotechnology applications. In this report, we were able to form distinct structures using pools of unique, chip-derived staple strands to fold scaffold strands in a denaturant-assisted one-pot anneal. Furthermore, an extended incubation step was added to the original anneal strategy to increase the yield of interconnected structures; this should be generalizable to larger multipart objects. The strategies presented here provide further pathways to increasing the scope of DNA nanotechnology.

METHODS

Reagents. The following materials and methods involving the inkjet printer and oligonucleotide synthesis have been reported previously and are briefly restated here for completeness.[16] Nucleoside phosphoramidites (Pac-dA-CE, Ac-dC-CE, iPr-Pac-dG-CE and dT-CE), 5-ethylthio-1*H*-tetrazole, Cap Mix A (5% phenoxyacetic anhydride in THF), and oxidizer (0.02 M iodine in pyridine/tetrahydrofuran/water) were purchased from Glen Research (Sterling, VA). Phosphoramidites and 5-ethylthio-1*H*-tetrazole were dissolved at 0.25 and 0.625 M, respectively, in a mixture of 50% 3-methoxypropionitrile and 50% glutaronitrile (Sigma, St. Louis, MO). The solvents were dried for 2 days on molecular sieves before use. Synthesis-grade anhydrous acetonitrile, Cap Mix B (*n*-methylimidazole in THF) and deblocking solution (dichloroacetic acid in DCM) were purchased from Azco Biotech (San Diego, CA). Purified M13 double-stranded plasmid and single-stranded phage were purchased from Bayou Biolabs (Metairie, LA). All other chemicals were purchased either from Sigma-Aldrich or VWR. Enzymes were from New England Biolabs.

Staple Complement Synthesis. Complementary versions of the required staple strands were synthesized atop cyclic olefin copolymer (COC) slides deposited with silica thin-film spots. In brief, prior to silica deposition, an array of microwells with bare COC bottom was created in a layer of photoresist, which was spin-coated on the COC slide surface using standard photolithographic techniques. Deposition of silica within the microwells was then performed as described elsewhere.[18,23] After deposition, the remaining photoresist was stripped by sonication in acetone. All patterned samples were immersed into a 1:1 H_2SO_4/H_2O_2 solution for 15 min to remove resist residue and finally rinsed with deionized water and blown dry. In the current design, COC slides were prepatterned to form eight subarrays of silica spots 150 μm in diameter and 300 μm in interfeature spacing (center-to-center). Each subarray contained 432 spots, and multiple spots were used to synthesize one oligo sequence. Complementary versions of staple strands were appended with a 25-base adaptor at the 3′ end, which provided a nicking site and anchored the oligo to the chip surface. All oligo sequences used in this study are listed in Supporting Information, section S3. *In situ* synthesis of DNA microarrays utilized standard phosphoramidite chemistry with a custom-built piezoelectric inkjet platform. A 1:1 mixture of methyl glutaronitrile (MGN) and 3-methoxypropionitrile (3MP) was used as solvent instead of volatile acetonitrile. Four channels on the printhead delivered phosphoramidite monomers (A, T, G, and C) and one delivered an activator (ethylthiotetrazole). Bulk reagents (*i.e.*, oxidizer, deprotection acid, acetonitrile, Cap A, Cap B) and waste were stored in glass bottles with GL-45 screw-top caps. Bulk reagents were controlled using PTFE solenoid valves leading to delivery lines colocated near the printhead (or to the slide holder for the waste line). Approximately 0.5 mL of each bulk reagent was added at a time, which was enough to cover the slide surface. An optical system was also colocated near the printhead, which captured high contrast images of printed droplets using a CCD detector and collimated LED light, enabling alignment of the printhead with a slide's silica features.

Each cycle of synthesis included (1) printing, (2) washing, (3) capping, (4) washing, (5) oxidation, (6) washing, (7) detritylation, and (8) displacement of detritylation reagent using oxidizer and

washing with acetonitrile. Slides were blown dry after each step (except printing) by a six-jet nitrogen manifold controlled by a solenoid valve. The first step of the reaction consisted of phosphoramidite monomer printing followed by tetrazole printing, and incubation for 2 min. The first base was reprinted four times with a 1-h incubation each time. Oxidization and capping were carried out for 30 s, whereas detritylation lasted 10 s. Washing after detritylation was done for 4 s but for only 2 s after every other step. After synthesis, the COC slides were removed from the synthesis platform and rinsed with acetonitrile and then 95% ethanol. The base-protecting groups were removed by a 2-h incubation in EDA/EtOH (anhydrous, 1:1 v/v) at room temperature. The deprotected slides were rinsed five times with deionized water, dried, and stored in a desiccator.

Nicking-Strand Displacement Amplification (nSDA) for on-Chip Staple Amplification and Purification. Printed COC slides were blocked using Pluronic F108 prior to amplification.[34,35] The chambers on the printed COC slides were filled with the nSDA reaction cocktail containing 0.4 mM dNTP, 0.2 mg/mL BSA, Nt.BstNBI, and Bst large fragment in optimized Thermopol II buffer supplemented with T4 Gene 32 protein. The slides with sealed chambers were placed on the slide adaptor of a Mastercycler Gradient thermocycler (Eppendorf) to carry out the nSDA reactions. Each amplification reaction involved incubation at 50 °C for 2 h after which the reaction was removed from the chip and denatured by heating at 80 °C for 20 min.

After the nSDA reaction, the amplified product from multiple chambers was pooled, and the DNA was then purified from proteinaceous material using the QuickClean Enzyme Removal Resin (Clontech) or by phenol−chloroform extraction, followed by ethanol precipitation, drying in a speed vacuum centrifuge (Eppendorf), and resuspension in sterile Milli-Q water.

For the assessment of nSDA, amplified product from a subarray containing 100, 75, or 50 microarrays (that presents approximately 4, 3, and 2 ng of template DNA, respectively, according to our previous surface density calculations[16]) synthesized with the sequence 5′-CGGTACCCGGGGATCCTCCAAATCGAAGGGATTTCGGAATTGTGGCGGGCATGACTCGACCATCCGATTTTTT-3′ was run on a 15% TBE−urea polyacrylamide gel. Incubation times of the nSDA were also varied from 5 min to 4 h. Gels were run with a low-weight mass estimation DNA ladder (Invitrogen). Fluorescent gel bands (from SYBR Gold staining) were then analyzed by AlphaImage software to yield estimates of amplified DNA.

Formation of DNA Origami. For the formation of tall rectangle, sharp triangle, and nanohouse DNA origami nanostructures, M13 single-stranded phage or M13 double-stranded plasmid and the appropriate synthesized staple strands (for the tall rectangle, sharp triangle, or nanohouse) were mixed together with a (1−10)-fold molar excess of staples. The concentrations of the scaffold strands as stated by the manufacturer (Bayou Biolabs) were used directly. The concentrations of the staple strand pools were determined as discussed in Supporting Information, section S1. Anneals were performed at 5 nM concentration of scaffold in 1 × TAE/Mg^{2+} buffer (40 mM Tris-HCl (pH 8.0), 20 mM acetic acid, 2 mM EDTA, and 12.5 mM magnesium acetate) with the designated percentage of formamide and heated to the designated initial temperature. Samples were quickly dropped to 25 °C and placed into 3.5 K MWCO Slide-A-Lyzer MINI dialysis units (Pierce Protein Research Products) and dialyzed at 10 min steps in buffered dialysant with the following formamide percentages: 33, 26, 20, 14, 7, and 0%. The additional 12-h incubation step to increase nanohouse formation yield was performed in a thermocycler at 30, 32.5, 35, 37, 40, 42.5, 45, 47.5, and 50 °C. The samples were incubated at 4 °C for at least 2 h before AFM imaging.

AFM Imaging of DNA Origami. An amount of 5 μL of DNA origami sample was deposited on freshly cleaved mica, followed by a 3-min wait before addition of 60 μL of 1 × TAE/Mg^{2+} buffer for tapping mode AFM analysis. AFM images were obtained on a Digital Instruments Nanoscope IIIa with a multimode head by tapping mode under buffer using DNP-10 or DNP-S10 silicone nitride tips (Veeco, Inc.).

Conflict of Interest: The authors declare no competing financial interest.

Acknowledgment. The authors wish to thank S. Zauscher for access to a Veeco Multimode Nanoscope IIIa atomic force microscope. This work was supported by Grants NSF-EMT-0829749, NSF-CCF-0835794, NSF-IRES-0965965, and ONR-N000140910249.

Supporting Information Available: Further details about annealing protocols, structure formation optimization, and oligonucleotide sequences. This material is available free of charge *via* the Internet at http://pubs.acs.org.

REFERENCES AND NOTES

1. Li, H.; LaBean, T. H.; Leong, K. W. Nucleic Acid-Based Nanoengineering: Novel Structures for Biomedical Applications. *Interface Focus* **2011**, *1*, 702–724.
2. Lin, C.; Yan, H. DNA Nanotechnology: A Cascade of Activity. *Nat. Nanotechnol.* **2009**, *4*, 211–212.
3. Rinker, S.; Ke, Y.; Liu, Y.; Chhabra, R.; Yan, H. Self-Assembled DNA Nanostructures for Distance-Dependent Multivalent Ligand-Protein Binding. *Nat. Nanotechnol.* **2008**, *3*, 418–422.
4. Gu, H. Z.; Chao, J.; Xiao, S. J.; Seeman, N. C. A Proximity-Based Programmable DNA Nanoscale Assembly Line. *Nature* **2010**, *465*, 202–205.
5. Voigt, N. V.; Torring, T.; Rotaru, A.; Jacobsen, M. F.; Ravnsbaek, J. B.; Subramani, R.; Mamdouh, W.; Kjems, J.; Mokhir, A.; Besenbacher, F.; *et al.* Single-Molecule Chemical Reactions on DNA Origami. *Nat. Nanotechnol.* **2010**, *5*, 200–203.
6. Rothemund, P. W. K. Folding DNA to Create Nanoscale Shapes and Patterns. *Nature* **2006**, *440*, 297–302.
7. Castro, C. E.; Kilchherr, F.; Kim, D. N.; Shiao, E. L.; Wauer, T.; Wortmann, P.; Bathe, M.; Dietz, H. A Primer to Scaffolded DNA Origami. *Nat. Methods* **2011**, *8*, 221–229.
8. Torring, T.; Voigt, N. V.; Nangreave, J.; Yan, H.; Gothelf, K. V. DNA Origami: A Quantum Leap for Self-Assembly of Complex Structures. *Chem. Soc. Rev.* **2011**, *40*, 5636–5646.
9. Pinheiro, A. V.; Han, D.; Shih, W. M.; Yan, H. Challenges and Opportunities for Structural DNA Nanotechnology. *Nat. Nanotechnol.* **2011**, *6*, 763–772.
10. Pilo-Pais, M.; Goldberg, S.; Samano, E.; Labean, T. H.; Finkelstein, G. Connecting the Nanodots: Programmable Nanofabrication of Fused Metal Shapes on DNA Templates. *Nano Lett.* **2011**, *11*, 3489–3492.
11. Douglas, S. M.; Dietz, H.; Liedl, T.; Hogberg, B.; Graf, F.; Shih, W. M. Self-Assembly of DNA into Nanoscale Three-Dimensional Shapes. *Nature* **2009**, *459*, 414–418.
12. Zhao, Z.; Liu, Y.; Yan, H. Organizing DNA Origami Tiles into Larger Structures Using Preformed Scaffold Frames. *Nano Lett.* **2011**, *11*, 2997–3002.
13. Hogberg, B.; Liedl, T.; Shih, W. M. Folding DNA Origami from a Double-Stranded Source of Scaffold. *J. Am. Chem. Soc.* **2009**, *131*, 9154–9155.
14. Zhang, H.; Chao, J.; Pan, D.; Liu, H.; Huang, Q.; Fan, C. Folding Super-Sized DNA Origami with Scaffold Strands from Long-Range PCR. *Chem. Commun.* **2012**, *48*, 6405–6407.
15. Carlson, R. The Changing Economics of DNA Synthesis. *Nat. Biotechnol.* **2009**, *27*, 1091–1094.
16. Saaem, I.; Ma, K. S.; Marchi, A. N.; LaBean, T. H.; Tian, J. D. *In Situ* Synthesis of DNA Microarray on Functionalized Cyclic Olefin Copolymer Substrate. *ACS Appl. Mater. Interfaces* **2010**, *2*, 491–497.
17. Kosuri, S.; Eroshenko, N.; LeProust, E. M.; Super, M.; Way, J.; Li, J. B.; Church, G. M. Scalable Gene Synthesis by Selective Amplification of DNA Pools from High-Fidelity Microchips. *Nat. Biotechnol.* **2010**, *28*, 1295–1299.
18. Tian, J.; Ma, K.; Saaem, I. Advancing High-Throughput Gene Synthesis Technology. *Mol. Biosyst.* **2009**, *5*, 714–722.
19. Lausted, C.; Dahl, T.; Warren, C.; King, K.; Smith, K.; Johnson, M.; Saleem, R.; Aitchison, J.; Hood, L.; Lasky, S. R. POSaM: A Fast, Flexible, Open-Source, Inkjet Oligonucleotide Synthesizer and Microarrayer. *Genome Biol.* **2004**, *5*, R58.
20. Quan, J.; Saaem, I.; Tang, N.; Ma, S.; Negre, N.; Gong, H.; White, K. P.; Tian, J. Parallel on-Chip Gene Synthesis and Application to Optimization of Protein Expression. *Nat. Biotechnol.* **2011**, *29*, 449–452.

21. Saaem, I.; Ma, K. S.; Tian, J. D. In Optimized in Situ DNA Synthesis on Patterned Glass. MRS Proceedings, Boston, Garrido, J. A., Johnston, E., Werner, C., Boland, T., Eds.; Materials Research Society: Boston, 2009.
22. Saaem, I.; Ma, K. S.; Alam, S. M.; Tian, J. D. Fabrication of Plastic Biochips. *J. Vac. Sci. Technol. A* **2010**, *28*, 963–968.
23. Kosuri, S.; Eroshenko, N.; LeProust, E. M.; Super, M.; Way, J.; Li, J. B.; Church, G. M. Scalable Gene Synthesis by Selective Amplification of DNA Pools from High-Fidelity Microchips. *Nat. Biotechnol.* **2010**, *28*, 1295–1299.
24. Joneja, A.; Huang, X. Linear Nicking Endonuclease-Mediated Strand-Displacement DNA Amplification. *Anal. Biochem.* **2011**, *414*, 58–69.
25. Kucera, R. Genome Amplification. Patent WO/2007/056173, 2007.
26. Tan, E.; Erwin, B.; Dames, S.; Ferguson, T.; Buechel, M.; Irvine, B.; Voelkerding, K.; Niemz, A. Specific *versus* Nonspecific Isothermal DNA Amplification through Thermophilic Polymerase and Nicking Enzyme Activities. *Biochemistry* **2008**, *47*, 9987–9999.
27. Jungmann, R.; Liedl, T.; Sobey, T.; Shih, W.; Simmel, F. Isothermal Assembly of DNA Origami Structures Using Denaturing Agents. *J. Am. Chem. Soc.* **2008**, *130*, 10062–10063.
28. Woo, S.; Rothemund, P. W. Programmable Molecular Recognition Based on the Geometry of DNA Nanostructures. *Nat. Chem.* **2011**, *3*, 620–627.
29. Andersen, E. S.; Dong, M.; Nielsen, M. M.; Jahn, K.; Lind-Thomsen, A.; Mamdouh, W.; Gothelf, K. V.; Besenbacher, F.; Kjems, J. DNA Origami Design of Dolphin-Shaped Structures with Flexible Tails. *ACS Nano* **2008**, *2*, 1213–1218.
30. Rajendran, A.; Endo, M.; Katsuda, Y.; Hidaka, K.; Sugiyama, H. Programmed Two-Dimensional Self-Assembly of Multiple DNA Origami Jigsaw Pieces. *ACS Nano* **2011**, *5*, 665–671.
31. Zuker, M. Mfold Web Server for Nucleic Acid Folding and Hybridization Prediction. *Nucleic Acids Res.* **2003**, *31*, 3406–3415.
32. Liu, W. Y.; Zhong, H.; Wang, R. S.; Seeman, N. C. Crystalline Two-Dimensional DNA-Origami Arrays. *Angew. Chem., Int. Ed.* **2011**, *50*, 264–267.
33. Samano, E. C.; Pilo-Pais, M.; Goldberg, S.; Vogen, B. N.; Finkelstein, G.; LaBean, T. H. Self-Assembling DNA Templates for Programmed Artificial Biomineralization. *Soft Matter* **2011**, *7*, 3240–3245.
34. Saaem, I.; Papasotiropoulos, V.; Wang, T.; Soteropoulos, P.; Libera, M. Hydrogel-Based Protein Nanoarrays. *J. Nanosci. Nanotechnol.* **2007**, *7*, 2623–2632.
35. Luk, V. N.; Mo, G. C. H.; Wheeler, A. R. Pluronic Additives: A Solution to Sticky Problems in Digital Microfluidics. *Langmuir* **2008**, *24*, 6382–6389.
36. McConaughy, B. L.; Laird, C. D.; McCarthy, B. J. Nucleic Acid Reassociation in Formamide. *Biochemistry* **1969**, *8*, 3289–3295.
37. Blake, R. D.; Delcourt, S. G. Thermodynamic Effects of Formamide on DNA Stability. *Nucleic Acids Res.* **1996**, *24*, 2095–2103.
38. Liedl, T.; Simmel, F. C. Determination of DNA Melting Temperatures in Diffusion-Generated Chemical Gradients. *Anal. Chem.* **2007**, *79*, 5212–5216.
39. Borovkov, A.; Loskutov, A.; Robida, M.; Day, Kristen.; Cano, J.; Le Olson, T.; Patel, H.; Brown, K.; Hunter, P.; Sykes, K. High-Quality Gene Assembly Directly from Unpurified Mixtures of Microarray-Synthesized Oligonucleotides. *Nucleic Acids Res.* **2010**, *38*, e180.